Journal of Computing and Information Science in Engineering | Volume 13 | Issue 2

Inverse Simulation under Uncertainty by Optimization

Xiaoping Du

Department of Mechanical and Aerospace Engineering
Missouri University of Science and Technology
400 West 13th Street, Toomey Hall 290D
Rolla, MO, 65406
Telephone: 573-341-7249
Email: dux@mst.edu

Abstract

Inverse simulation is an inverse process of a direct simulation. During the process, unknown simulation input variables are identified for a given set of known simulation output variables. Uncertainties such as random parameters may exist in engineering applications of inverse simulation. An optimization method is developed in this work to estimate the probability distributions of unknown input variables. The First Order Reliability Method is employed and modified so that the inverse simulation is embedded within the reliability analysis. This treatment avoids the separate executions of reliability analysis and inverse simulation and consequently maintains high efficiency. In addition, the means and standard deviations of the unknown input variables can also be obtained. A particle impact problem is presented to demonstrate the proposed method for inverse simulation under uncertainty.

1. Introduction

Simulations are widely used in engineering analysis and design. They can evaluate potential design alternatives and predict design performances efficiently and inexpensively. The conventional simulation is a forward process where the behavior (simulation output) of a system under design is found from a given model structure and a set of model input variables.

The direct or forward simulation is not the only simulation approach to complex engineering analysis and design. The development of inversing the process began in the 1960s and 1970s with a class of methods termed dynamic inversion or feedback linearization for multivariable nonlinear minimum-phase systems [1]. The methodologies of inverse simulation were then expanded in areas of aircraft flight control and aircraft handling quality investigations [2], where inverse simulation is defined as "a form of inverse modelling in which computer simulation methods are used to find the time histories of input variables that, for a given model, match a set of required output responses" [2]. The applications of inverse simulation include the following examples: flight dynamics [3], the optimization of a helicopter slalom maneuver [4], the flight simulation for a fatigue life management system [5], the helicopter simulation with an enhanced rotor model [6], and the analysis of the orbit plane change of a spacecraft [7].

Another important area of inverse simulation is inverse dynamics, whose purpose is to determine forces or toques needed to produce desired motions [8-9]. For example, in biomechanics, certain human movements are desired, and the inverse dynamics is used to determine the joint torques and powers that a human body must generate to perform the movements. The other related technique is inverse kinematics. This technique uses

kinematics equations of a robot to determine the joint parameters that provide a desired position of the end-effector [10]. Here the end effector is a device at the end of a robotic arm, designed to interact with the environment.

The inverse simulation techniques can be potentially used in almost all areas where the direct simulation technique is applicable. We can then define inverse simulation as a process where computer simulation methods are used to find a set of model input variables that realize a set of required model output responses. In this sense, in addition to the aforementioned inverse simulations, many other applications fall into the scope of inverse simulation.

For example, traffic accident reconstruction [11-14] involves inverse simulation techniques. Its purpose is to investigate, analyze, and draw conclusions about the causes and events of a vehicle collision. Specifically, a collision analysis is performed to identify the contributing factors to the collision, including the role of the drivers, vehicles, road conditions, and environment. The modeling and analysis are complicated because they usually require the use of momentum, work and energy principles, and kinematics. As a result, the use of a numerical simulation is necessary. Traffic accident reconstruction is an inverse process of simulation because it reconstructs the pre-accident events given the accident consequences.

As many uncertainties present in the direct process of simulations [15-22], we also face uncertainties in inverse simulations. The uncertainties may come from simulation parameters due to the random physical nature, manufacturing imprecision, random operating conditions, and measurement errors; they can also come from model structure uncertainties due to simplifications, assumptions, ignorance, and lack of information. For

example, there are many sources of uncertainty in traffic accident reconstruction as reported in [23-24].

With the uncertainties mentioned above, the estimated simulation input variables from the inverse simulation will also be uncertain. Obtaining the uncertainty characteristics, such as the distributions, means, and standard deviations, of the input variables, are highly desired.

For instance, a basic expectation of the inverse vehicle accident simulation is to find the velocities of the vehicles prior to collision and then assess the drivers' behavior. The simulation results may be used as part of evidence for the court to make its decision on the responsibility of the involving drivers. The consideration of uncertain helps build confidence in the results of the traffic accident reconstruction.

Instead of point estimations, the distributions of the unknown input variables are available from the inverse simulation under uncertainty. With the more information and higher confidence from the uncertainty consideration, the model user or a decision maker will have a better position to make more reliable decisions.

The other advantage of inverse simulation under uncertainty is that the simulation results can be directly used for risk-related analysis, such as the analyses regarding safety, reliability, and robustness. These analyses normally require probability distributions. The results are also useful for risk-based design, reliability-based design, robust design, design for Six Sigma, and alike.

Unlike direct simulation under uncertainty, for which many methodologies are available, methodologies for inverse simulation under uncertainty are limited. Although preliminary studies in vehicle inverse simulation have been reported [23-24], more

investigations are needed. In this work, we build a new probabilistic model for the inverse simulation under uncertainty and then develop a reliability approach to solve the inverse simulation model. The approach integrates the First Order Reliability Method (FORM) and the general inverse simulation process in such a manner so that the inverse simulation under uncertainty can be efficiently performed. This is achieved by embedding the inverse simulation process within the FORM algorithm. Given a set of output variables, along with the distributions of a set of uncertain input variables, the distributions of the unknown input variables are obtained. An example of particle impact is presented as a demonstration for the proposed model.

2. Problem Formulation

Fig. 1 shows a general simulation model with its input $\mathbf{x}$ (a vector) and output $\mathbf{y}$ (a vector as well). The simulation model $\mathbf{g}(\mathbf{x})$ maps $\mathbf{x}$ into $\mathbf{y}$ and is usually a black box to the model user. For a direct simulation, the output $\mathbf{y}$ is found through $\mathbf{g}(\mathbf{x})$ with the input $\mathbf{x}$. For the inverse simulation, the output $\mathbf{y}$ is known, and the task is to search for the input $\mathbf{x}$.

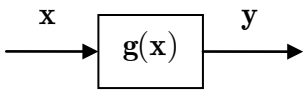

Figure 1. A simulation model

The general simulation model is given by

$$\mathbf{y} = \mathbf{g}(\mathbf{x}) \tag{1}$$

or

$$\begin{cases} y_1 = g_1(\mathbf{x}) \\ y_2 = g_2(\mathbf{x}) \\ \cdots \\ y_m = g_m(\mathbf{x}) \end{cases} \tag{2}$$

where $\mathbf{y} = (y_1, \ldots, y_m)$ with a size of m, and $\mathbf{g}(\cdot) = (g_1(\cdot), \ldots g_m(\cdot))$.

Inverse simulation problems fall into the following three categories [5]:

- problems in which the size of $\mathbf{x}$ is equal to that of $\mathbf{y}$,
- problems in which the size of $\mathbf{x}$ exceeds that of $\mathbf{y}$, and
- problems in which the size of $\mathbf{x}$ is smaller than that of $\mathbf{y}$.

The number of unknowns is equal to the number of equations for a problem in the first category. A unique (single) solution or multiple solutions may exist. The number of unknowns is greater than the number of equations for a problem in the second category. There may be multiple solutions to the problem. Since the number of unknowns is less than the number of equations, no solutions may be found for a problem in the last category. In this work, we focus on the problems in the first category where a unique solution exists for an inverse simulation problem.

For inverse simulation, the output $\mathbf{y}$ is known for several reasons. For instance, we may want to achieve specific target values of $\mathbf{y}$. An example follows. The motion output of a robot is the position of its finger. We expect the finger to reach specified positions. So we can set up the specified position coordinates for $\mathbf{y}$. Another example follows. If an inverse simulation intends to reconstruct a vehicle accident, $\mathbf{y}$ can be the variables associated with the accident consequences and may be measured at the accident scene. In

this work, we assume that we know the output $\mathbf{y}$ beforehand. We also further assume that the values of $\mathbf{y}$ are deterministic.

The task of inverse simulation is then to find input variables $\mathbf{x}$ to match $\mathbf{y}$. Since not all the input variables are unknown, we classify them into two types: known input variables and unknown input variables.

Some of the known input variables may be precisely known. For example, the weights of the two vehicles involved in an accident can be measured and then are precisely known if their measurement errors are negligible. For those variables, we use $\mathbf{x}_{\mathrm{kn}}$. We also assume that they are deterministic.

Other known input variables, however, may not be precisely known, or may be uncertain. For example, for the vehicle accident simulation, the coefficient of friction may be a random variable. It depends on many random factors, such as the wear of tires, road conditions, and weather. We denote these uncertain variables by $\mathbf{x}_{\mathrm{unc}}$. In this work, we assume that distributions $\mathbf{x}_{\mathrm{unc}}$ are known. For a specific inverse simulation problem, the deterministic realizations of $\mathbf{x}_{\mathrm{unc}}$ are actually involved. But it may be difficult to determine those realizations. In this case, $\mathbf{x}_{\mathrm{unc}}$ are still treated uncertain. It is the case that is concerned by this work.

We use $\mathbf{x}_{\mathrm{unkn}}$ to represent those input variables that are to be determined from the inverse simulation. For example, in the inverse simulation for traffic accident reconstruction, the initial velocities of two vehicles that were involved in an accident could be part of $\mathbf{x}_{\mathrm{unkn}}$.

Then the input variables $\mathbf{x}$ are

$$\mathbf{x} = (\mathbf{x}_{\text{unkn}}, \mathbf{x}_{\text{kn}}, \mathbf{x}_{\text{unc}}) \tag{3}$$

where

$\mathbf{x}_{\text{unkn}} = (x_{\text{unkn},1}, \ldots, x_{\text{unkn},n_1})$ with a size of n_1,

$\mathbf{x}_{\text{kn}} = (x_{\text{kn},1}, \ldots, x_{\text{kn},n_2})$ with a size of n_2, and

$\mathbf{x}_{\text{unc}} = (x_{\text{unc},1}, \ldots, x_{\text{unc},n_3})$ with a size of n_3.

Then the simulation model is

$$\mathbf{y} = \mathbf{g}(\mathbf{x}_{\text{unkn}}, \mathbf{x}_{\text{kn}}, \mathbf{x}_{\text{unc}}) \tag{4}$$

The task of inverse simulation is to find unknown input variables $\mathbf{x}_{\text{unkn}}$ given the output variables $\mathbf{y}$ and known input variable $(\mathbf{x}_{\text{kn}}, \mathbf{x}_{\text{unc}})$. Since $\mathbf{x}_{\text{unkn}}$ depends on random input variables $\mathbf{x}_{\text{unc}}$, $\mathbf{x}_{\text{unkn}}$ may be random. It is desirable to obtain the distributions of $\mathbf{x}_{\text{unkn}}$. As a result, our proposed model for inverse simulation under uncertainty is established as follows:

Given:	CDF of $x_{\text{unc},i}$ $(i = 1, \ldots, n_3)$ $F_{\text{unc},i}(x)$,
	$\mathbf{x}_{\text{kn}} = (x_{\text{kn},1}, \ldots, x_{\text{kn},n_2})$,
	$\mathbf{y} = (y_1, \ldots, y_m)$, and
	$\mathbf{g}(\cdot) = (g_1(\cdot), \ldots g_m(\cdot))$
Find:	CDF of $x_{\text{unkn},j}$ $(j = 1, \ldots, n_1)$
	$F_{\text{unkn},j}(x)$

where the CDF stands for the cumulative distribution function.

The uncertainty analysis, which is responsible for solving the above model, needs a number of inverse simulations. In general, an inverse simulation also requires a number of direct simulations. Mathematically, an inverse simulation is equivalent to the process of solving the following system of simultaneous equations:

$$\begin{cases} y_1 = g_1((x_{\text{unkn},1},\ldots,x_{\text{unkn},n_1}),\mathbf{x}_{\text{kn}},\mathbf{x}_{\text{unc}}) \\ y_2 = g_2((x_{\text{unkn},1},\ldots,x_{\text{unkn},n_1}),\mathbf{x}_{\text{kn}},\mathbf{x}_{\text{unc}}) \\ \ldots \\ y_m = g_m((x_{\text{unkn},1},\ldots,x_{\text{unkn},n_1}),\mathbf{x}_{\text{kn}},\mathbf{x}_{\text{unc}}) \end{cases} \tag{5}$$

For the problems in the first category, $n_1 = m$, a general iterative procedure of inverse simulation is shown in Fig. 2.

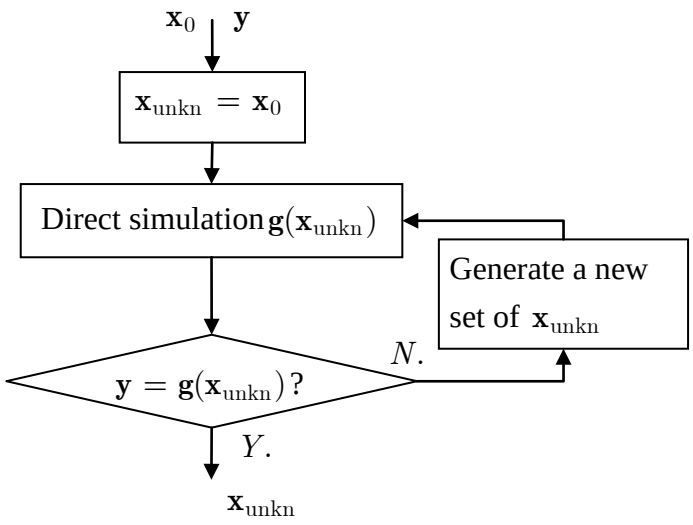

Figure. 2 Flowchart of inverse simulation

3. Reliability Approach to Inverse Simulation

As discussed above, the computation of the inverse simulation under uncertain may be intensive because many direct simulations are needed. The Monte Carlo simulation (MCS) is not a good choice for such a task if the direct simulation is expensive. Our

interest is to develop an efficient approach so that the inverse simulation under uncertainty is affordable. Our strategy is to use a reliability analysis method for such a task. This is possible because the evaluation of the CDF of an unknown input variable is the same task as the reliability analysis.

Let a general component in $\mathbf{x}_{\text{unkn}}$ be x_{unkn}. Its CDF is defined by

$$F_{\text{unkn}}(x) = \Pr(x_{\text{unkn}} < x) \tag{6}$$

The CDF can be obtained from reliability analysis, during which the inverse simulation is called repeatedly. Many reliability analysis methods require an iterative or optimization process, such as the First Order Reliability Method (FORM) [25-27], the Second Order Reliability Method (SORM) [28], the First Order Saddlepoint Approximation (FSA) method [29-31], and the First Order Second Moment Method (FOSM) [32]. All of those methods need to call the inverse simulation several times to obtain the derivatives of x_{unkn} with respect to the random input variables $\mathbf{x}_{\text{unc}}$. To ensure acceptable accuracy, sampling-based methods such as MCS must also call the inverse simulation with sufficient number of times, and usually the number of inverse simulations is much higher than the aforementioned methods. Therefore, the computational cost is a major concern. Since FORM has good balance between accuracy and efficiency, we use FORM in this work.

3.1 Integrate FORM and inverse simulation

FORM transforms $\mathbf{x}_{\text{unc}}$ into independent random variables $\mathbf{u} = (u_1, \ldots, u_{n_3})$, where u_i ($i = 1, \ldots, n_3$) follows a standard normal distribution. Then the simulation model becomes

$$y = g(\mathbf{x}_{\text{unkn}}, \mathbf{x}_{\text{kn}}, \mathbf{x}_{\text{unc}}) = g(\mathbf{x}_{\text{unkn}}, \mathbf{x}_{\text{kn}}, \mathrm{T}(\mathbf{u})) \tag{7}$$

where y and $g(\cdot)$ are a general component of $\mathbf{y}$ and $\mathbf{g}(\cdot)$, respectively. $\mathrm{T}(\cdot)$ denotes the transformation. Combining FORM with the inverse simulation, we can then obtain the CDF of x_{unkn} with the following equations:

If $x_{\text{unkn}} \le x$ when $\mathbf{u} = (0,\ldots,0)$

$$F_{\text{unkn}}(x) = \Pr(x_{\text{unkn}} < x) = \Phi(\beta) \tag{8}$$

where $\Phi(\cdot)$ is the CDF of a standard normal variable, and

$$\beta = \left\| \mathbf{u}^* \right\| = \left(\sum_{i=1}^{n_3} (u_i^*)^2 \right)^{0.5} \tag{9}$$

in which $\left\| \cdot \right\|$ stands for a L-2 norm of a vector, and $\mathbf{u}^* = (u_1^*,\ldots,u_{n_3}^*)$ is the Most Probable Point [27] obtained from the following optimization:

$$\begin{cases} \min\limits_{\mathbf{u}} \quad \beta = \left\| \mathbf{u} \right\| \\ \text{subject to} \\ x_{\text{unkn}} = g^{-1}(\mathbf{x}_{\text{unkn}}, \mathbf{x}_{\text{kn}}, \mathrm{T}(\mathbf{u})) \le x \end{cases} \tag{10}$$

$g^{-1}(\cdot)$ is the function of x_{unkn} and is numerically attainable from the inverse simulation.

If $x_{\text{unkn}} > x$ when $\mathbf{u} = (0,\ldots,0)$

$$F_{\text{unkn}}(x) = \Pr(x_{\text{unkn}} < x) = 1 - \Phi(\beta) \tag{11}$$

where β is computed with Eq. (9), and $\mathbf{u}^*$ is obtained from the following optimization

$$\begin{cases} \min\limits_{\mathbf{u}} \quad \beta = \left\| \mathbf{u} \right\| \\ \text{subject to} \\ x_{\text{unkn}} = g^{-1}(\mathbf{x}_{\text{unkn}}, \mathbf{x}_{\text{kn}}, \mathrm{T}(\mathbf{u})) > x \end{cases} \tag{12}$$

During the MPP search optimization process, the inverse simulation needs to be called in order to obtain $g^{-1}(\cdot)$ at each intermediate point and the initial point of $\mathbf{u}$. This means that the inverse simulation process in Eq. (5) is an inner loop that is embedded in the reliability outer loop in Eq. (10) or (12). This direct integration of FORM and inverse simulation is therefore a double-loop process and may be computationally expensive. The double-loop procedure is illustrated in Fig. 3.

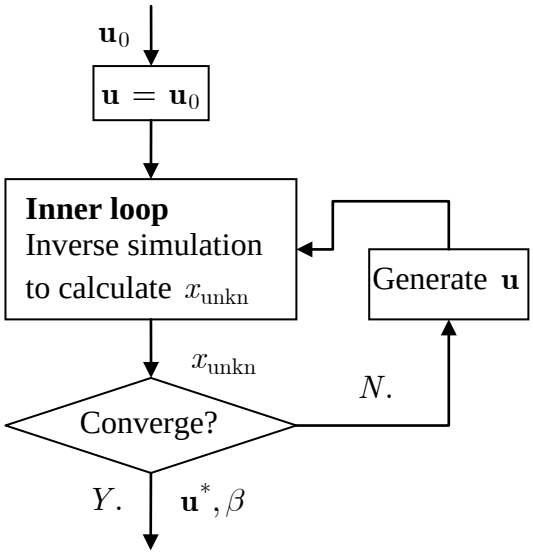

Figure. 3 Double-loop procedure for inverse simulation under uncertainty

Next we develop an efficient computational model that eases the computational burden.

3.2 Efficient integration of FORM and inverse simulation

To eliminate the embedded double-loop procedure mentioned above, we move the system of equations of the inverse simulation in Eq. (5) into the reliability analysis optimization model. We treat these equations as equality constraints. To ensure a true

solution to both the reliability analysis and inverse simulation, we also include the unknown variables $\mathbf{x}_{\text{unkn}}$ as additional design variables in the reliability analysis model. As a result, the design variables are now $(\mathbf{u}, \mathbf{x}_{\text{unkn}})$. With this treatment, the overall inverse simulation under uncertainty becomes a single-loop procedure. The new models of the inverse simulation under uncertainty are then developed as follows:

If $x_{\text{unkn}} \le x$ when $\mathbf{u} = (0,\ldots,0)$, the new model is

$$\begin{cases} \min\limits_{(\mathbf{u},\mathbf{x}_{\text{unkn}})} \beta = \left\|\mathbf{u}\right\| \\ \text{subject to} \\ x_{\text{unkn}} \le x \\ \mathbf{y} = \mathbf{g}(\mathbf{x}_{\text{unkn}}, \mathbf{x}_{\text{kn}}, T(\mathbf{u})) \end{cases} \tag{13}$$

where $\mathbf{g}(\cdot) = (g_1(\cdot),\ldots, g_{n_3}(\cdot))$.

If $x_{\text{unkn}} > x$ when $\mathbf{u} = (0,\ldots,0)$, the new model is

$$\begin{cases} \min\limits_{(\mathbf{u},\mathbf{x}_{\text{unkn}})} \beta = \left\|\mathbf{u}\right\| \\ \text{subject to} \\ x_{\text{unkn}} > x \\ \mathbf{y} = \mathbf{g}(\mathbf{x}_{\text{unkn}}, \mathbf{x}_{\text{kn}}, T(\mathbf{u})) \end{cases} \tag{14}$$

The above models indicate three modifications of FORM: (1) The design space is expanded from $\mathbf{u}$ to $(\mathbf{u}, \mathbf{x}_{\text{unkn}})$; (2) new constraint functions $\mathbf{y} = \mathbf{g}(\mathbf{x}_{\text{unkn}}, \mathbf{x}_{\text{kn}}, T(\mathbf{u}))$ are added; and (3) the inverse simulation for $g^{-1}(\cdot)$ is eliminated.

With the new models, the MPP search and the system of inverse simulation equations are totally combined. There is no need to perform a complete inverse simulation at each updated point during the MPP search. Only direct simulations are conducted. The new models then involve only a single-loop procedure, and the computational efficiency is

therefore much higher than that of the double-loop procedure. The single-loop procedure is illustrated in Fig. 4.

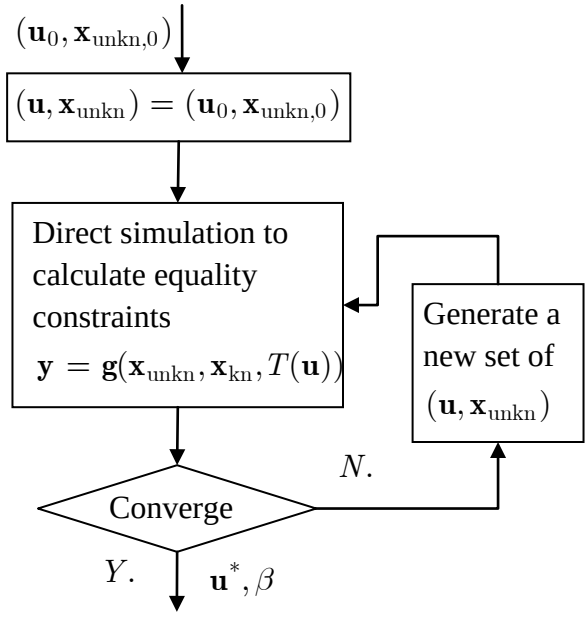

Figure. 4 Single-loop procedure for inverse simulation under uncertainty

The solutions from the new model can be proved to be also the solutions to the double-loop model and therefore to be the true solutions to the inverse simulation under uncertainty. The proof is given in the next subsection.

The procedure of the propose method is summarized below.

(1) Let $i = 1$, where i is the index for the unknown input variables $\mathbf{x}_{\text{unkn}}$.

(2) Let $x_{\text{unkn}} = x_{\text{unkn},i}$, where $\mathbf{x}_{\text{unkn},i}$ is the *i*-th component of $\mathbf{x}_{\text{unkn}}$.

(3) Perform the inverse simulation under uncertainty by the MPP search in Eq. (13) or (14).

a. Call direct simulation $\mathbf{y} = \mathbf{g}(\mathbf{x}_{\text{unkn}}, \mathbf{x}_{\text{kn}}, T(\mathbf{u}))$ and evaluate $\beta = \left\|\mathbf{u}\right\|$ at $(\mathbf{u}, \mathbf{x}_{\text{unkn}})$.

b. Update $(\mathbf{u}, \mathbf{x}_{\text{unkn}})$.

c. Check convergence. If convergence is reached, exit step (3); otherwise, repeat this step.

(4) Calculate the CDF of x_{unkn} by Eq. (8) or (11).

(5) Repeat steps (1) through (4) until $i = n_3$.

3.3 Moment estimation

After the CDF $F_{\text{unkn}}(x)$ is obtained, we can also estimate the moments of x_{unkn}. For example, the mean of x_{unkn} is given by

$$\mu = \int_{-\infty}^{\infty} x f_{\text{unkn}}(x) dx = \int_{-1}^{1} x dF_{\text{unkn}}(x) \tag{15}$$

where $f_{\text{unkn}}(x)$ is the probability density function (PDF) of x.

Let $w = F_{\text{unkn}}(x)$, μ becomes

$$\mu = \int_{-1}^{1} x_w dw \tag{16}$$

where x_w is the percentile value of x_{unkn} and is given by

$$F_{\text{unkn}}(x_w) = w \tag{17}$$

or

$$x_w = F_{\text{unkn}}^{-1}(w) \tag{18}$$

Then

$$\mu = \int_{-1}^{1} x_w dw \tag{19}$$

Similarly, the variance of x_{unkn} can be estimated by

$$\sigma^2 = \int_{-\infty}^{\infty} x^2 f_{\text{unkn}}(x)dx - \mu^2 = \int_{-1}^{1} x_w^2 dw - \mu^2 \tag{20}$$

To obtain the two moments, we need to obtain the percentile value $x_w = F^{-1}(w)$. x_w can be easily evaluated by modifying the models in Eqs. (13) and (14) [17].

If $w < 0.5$, $\beta = -\Phi^{-1}(w)$, then x_w is the solution to the following model:

$$\begin{cases} \max\limits_{(\mathbf{u},\mathbf{x}_{\text{unkn}})} x_{\text{unkn}} \\ \text{subject to} \\ \left\| \mu \right\| = \beta \\ \mathbf{y} = \mathbf{g}(\mathbf{x}_{\text{unkn}}, \mathbf{x}_{\text{kn}}, \text{T}(\mathbf{u})) \end{cases} \tag{21}$$

If $w > 0.5$, $\beta = \Phi^{-1}(w)$, then x_w is the solution to the following model:

$$\begin{cases} \min\limits_{(\mathbf{u},\mathbf{x}_{\text{unkn}})} x_{\text{unkn}} \\ \text{subject to} \\ \left\| \mu \right\| = \beta \\ \mathbf{y} = \mathbf{g}(\mathbf{x}_{\text{unkn}}, \mathbf{x}_{\text{kn}}, \text{T}(\mathbf{u})) \end{cases} \tag{22}$$

The procedure of the evaluation of x_w is similar to that of the CDF of x_{unkn}. The steps are therefore omitted.

μ and σ^2 can be evaluated by a numerical integration method. The evaluation needs to call the above two models a number of times.

3.4 Proof

It can be proved that the proposed models in Eqs. (13) and (14) generate solutions that satisfy both the original reliability models in Eqs. (10) and (12), and the inverse

simulation model in Eq. (5). The proof is based on the Karush–Kuhn–Tucker (KKT) conditions. The KKT conditions are necessary conditions, which state that if a solution (point) is optimal, then it satisfies the KKT conditions. The true optimal point is among all the points that satisfy the KKT conditions. We show that the proposed single-loop procedure results in the same points that satisfy the KKT conditions. The other reason we use the KKT conditions is that they are commonly employed in the popular MPP search algorithms and many optimization algorithms.

Assume that the unknown variable x_{unkn} is a general component of $\mathbf{x}_{\text{unkn}}$. Define the Lagrangian function for the MPP search in Eq. (10) as

$$L = \beta + ex_{\text{unkn}} \tag{23}$$

where e is a constant. Using $\nabla L = \mathbf{0}$ (∇ denotes a gradient), we have the following KKT conditions:

$$\begin{cases} \nabla\beta + e\nabla x_{\text{unkn}} = 0 \\ x_{\text{unkn}} \le x \\ e \ge 0 \end{cases} \tag{24}$$

The KKT conditions can then be rewritten as

$$\begin{cases} \dfrac{\mathbf{u}}{\beta} + e\left(\dfrac{\partial x_{\text{unkn}}}{\partial u_i}\right)_{i=1,\ldots n_3} = 0 \\ x_{\text{unkn}} \le x \\ e \ge 0 \end{cases} \tag{25}$$

In the above equation, we use the following notation for a vector: $\mathbf{a} = (a_1, \ldots \mathrm{a}_n) = (a_i)_{i=1}^n$.

We consider that the inverse simulation in Eq. (5) is also an optimization problem. This optimization problem has a constant objective c, and the Lagrangian function is then given by

$$L = c + \sum_{i=1}^{n_1} \lambda_i g_i \tag{26}$$

where λ_i $(i = 1,\ldots n_1)$ are constant.

The KKT conditions are

$$\begin{cases} \sum_{i=1}^{n_1} \lambda_i \left(\dfrac{\partial g}{\partial x_{\text{unkn},i}} \right)_{i=1}^{n_1} = 0 \\ y_j = g_j,\ j = 1,\ldots,n_1 \end{cases} \tag{27}$$

If we can approve that the KKT conditions of the proposed model in Eq. (13) or (14) produces the KKT conditions of the reliability analysis in Eq. (10) or (12) and those of the inverse simulation in Eq. (5), then the proposed models do produce solutions to both the reliability analysis and inverse simulation. The Lagrangian function of the proposed model in Eq. (13) is

$$L = \beta + e x_{\text{unkn}} + \sum_{i=1}^{n_1} \lambda_i g_i \tag{28}$$

And the KKT conditions are

$$\begin{cases} \dfrac{\mathbf{u}}{\beta} + e \left(\dfrac{\partial x_{\text{unkn}}}{\partial u_i} \right)_{i=1}^{n_3} + \sum_{k=1}^{n_1} \lambda_k \left(\dfrac{\partial g_k}{\partial u_j} \right)_{j=1}^{n_3} = 0 \\ \sum_{k=1}^{m} \lambda_k \left(\dfrac{\partial g}{\partial x_{\text{unkn},j}} \right)_{j=1}^{n_3} = 0 \\ x_{\text{unkn}} \le x \\ e \ge 0 \\ y_j = g_j,\ j = 1,\ldots n_1 \end{cases} \tag{29}$$

The second line and last line give the KKT conditions of the inverse simulation as shown in Eq. (28). This indicates that the proposed model in Eq. (13) satisfies the conditions imposed to the inverse simulation.

Using the inverse simulation equations in Eq. (5) $y_k = g_k((x_{\text{unkn},1},\ldots,x_{\text{unkn},n_1}),\mathbf{x}_{\text{kn}},\mathrm{T}(\mathbf{u}))$ ($k = 1,\ldots,n_1$), we obtain

$$\frac{\partial g_k}{\partial x_{\text{unkn}}}\frac{\partial x_{\text{unkn}}}{\partial u_i} + \frac{\partial g_k}{\partial u_i} = 0 \tag{30}$$

with $i = 1,\ldots n_3$. Then

$$\frac{\partial g_k}{\partial u_i} = -\frac{\partial g_k}{\partial x_{\text{unkn}}}\frac{\partial x_{\text{unkn}}}{\partial u_i} \tag{31}$$

Plugging the above equation into the first line in Eq. (29) yields

$$\frac{\mathbf{u}}{\beta} + \left(e - \sum_{k=1}^{n_1}\lambda_k \frac{\partial g_k}{\partial x_{\text{unkn}}}\right)\left(\frac{\partial x_{\text{unkn}}}{\partial u_i}\right)_{j=1}^{n_3} = 0 \tag{32}$$

Since $\sum_{k=1}^{n_1}\lambda_k \frac{\partial g_k}{\partial x_{\text{unkn}}} = 0$ from Eq. (27), the above equation becomes

$$\frac{\mathbf{u}}{\beta} + e\left(\frac{\partial x_{\text{unkn}}}{\partial u_i}\right)_{i=1,\ldots n_3} = 0 \tag{33}$$

which is the same equation as the first line of the KKT conditions of the reliability analysis in Eq. (25). The first line and the fourth line of the KKT conditions of the proposed model in Eq. (13) produce the same KKT conditions of the reliability analysis. This completes the proof.

The process of proofing the other proposed model in Eq. (14) is similar, and the proof is omitted.

4. EXAMPLE

We now present an example to show the application of the proposed method. It is an impact problem involving two rigid bodies as shown in Fig. 5. The ball *A* with an initial velocity v_{A0} strikes the block *B* as it travels down the inclined plane at a velocity v_{B0} as shown. After collision, block *B* slides up the inclined plane for a distance d_B where it momentarily stops as shown by the dotted block. The ball bounces back along the dotted path and hits floor with a horizontal distance d_A.

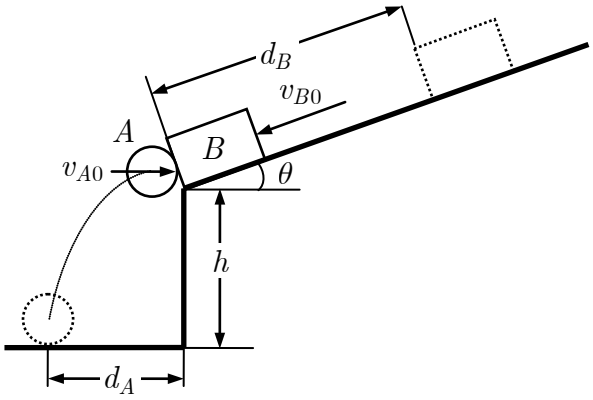

Figure. 5 Impact of two rigid bodies

The impact problem can be simulated with dynamics simulation software, such as ADAMS, which is the widely used multi-body dynamics and motion analysis software. The input variables include the initial velocities of the two bodies, v_{A0} and v_{B0}, and the simulation output variables are the distances d_A and d_B.

If the collision is considered as an accident, we are then interested in reconstructing the accident. The results of the accident, such as the distances d_A and d_B, can be easily

measured at the accident scene. The basic question then could be: What are the velocities of the two bodies just before collision? This requires an inverse simulation where we know the simulation output d_A and d_B, and we would like to find simulation input v_{A0} and v_{B0}.

Since our purpose is an easy methodology demonstration, we simplify the simulation model by treating the two bodies as two particles. With this assumption, equations for the simulation can be derived from particle dynamics. The equations are given in the Appendix. To mimic the real application of the inverse process of a direct simulation, however, we assume that the equations are invisible to a model user; in other words, the simulation model is a black box. As a result, to obtain the simulation input by the inverse simulation, we need to perform a number of direct simulations as indicated in Eq. (5) and Fig. 1.

The settings of the inverse simulations are as follows:

(1) Simulation input variables $\mathbf{x} = (\mathbf{x}_{\text{unkn}}, \mathbf{x}_{\text{kn}}, \mathbf{x}_{\text{unc}})$

The unknown input variables are the initial velocities of the two bodies v_{A0} and v_{B0}, i.e., $\mathbf{x}_{\text{unkn}} = (v_{A0}, v_{B0})$.

The known input variables include the masses of the two bodies $m_A = 2$ kg, $m_B = 6$ kg, the height $h = 2$ m, and the angle $\theta = 20^\circ$. Therefore, $\mathbf{x}_{\text{kn}} = (m_A, m_B, h, \theta)$.

The uncertain input variables are the coefficient of restitution e and coefficient of friction between the block and the inclined plane μ_k. The two coefficients are determined by many random factors such as the material properties, the surface roughness, and the

weather conditions. They can be estimated with probability distributions. We assume that the two variables are independently and normally distributed. Their means are 0.6 and 0.4, respectively, and their standard deviations are 0.06 and 0.04, respective. Then $\mathbf{x}_{\text{unc}} = (e, \mu_k)$. For a specific impact problem, the two variables are uniquely determined. In other words, they are a realization of $\mathbf{x}_{\text{unc}} = (e, \mu_k)$ and therefore deterministic. However, it is hard to measure the values of the two variables. Hence we still treat them as uncertain variables and use their distributions. Due to the uncertainties in the two variables, the unknown simulation input variables will be also uncertain even though their actual values are deterministic.

(2) Simulation output variables $\mathbf{y}$

The output variables include the distances d_A and d_B, or $\mathbf{y} = (d_A, d_B)$. We assume that the two variables are obtained from measurement and that $d_A = 0.582$ m and $d_B = 0.708$ m.

(3) Simulation model $\mathbf{y} = \mathbf{g}(\mathbf{x}_{\text{unkn}}, \mathbf{x}_{\text{kn}}, \mathbf{x}_{\text{unc}})$

$\mathbf{y} = (d_A, d_B) = (g_1(\mathbf{x}_{\text{unkn}}, \mathbf{x}_{\text{kn}}, \mathbf{x}_{\text{unc}}), g_2(\mathbf{x}_{\text{unkn}}, \mathbf{x}_{\text{kn}}, \mathbf{x}_{\text{unc}}))$. $g_1(\cdot)$ and $g_2(\cdot)$ are given in the Appendix and are assumed to be black boxes to a model user. It is noted that the two models are nonlinear functions with respect to $\mathbf{x}_{\text{unkn}}$ and $\mathbf{x}_{\text{unc}}$.

The accuracy of the new method is verified by Monte Carlo simulation (MCS). The procedure of the MCS for a general input variable x_{unkn} is summarized below.

(1) Let $i = 1$.

(2) Obtain samples of random variables $\mathbf{x}_{\text{unc},i}$, the *i*-th sample of $\mathbf{x}_{\text{unc}}$, from the distributions of $\mathbf{x}_{\text{unc}}$. Then form the input variables $\mathbf{x}_i = (\mathbf{x}_{\text{unkn},i}, \mathbf{x}_{\text{kn}}, \mathbf{x}_{\text{unc},i})$

(3) Solve for the unknown input variables $\mathbf{x}_{\text{unkn}}$ and obtain the sample $x_{\text{unkn},i}$ with the equations of the inverse simulation $\mathbf{y} = \mathbf{g}(\mathbf{x}_i) = g(\mathbf{x}_{\text{unkn},i}, \mathbf{x}_{\text{kn}}, \mathbf{x}_{\text{unc},i})$.

(4) Repeat steps (2) and (3) until $i = N$, where N is the number of simulations.

(5) Perform statistics analysis to obtain the CDF, mean, and standard deviation of the unknown input variable x_{unkn}.

In step (5), the CDF is estimated by

$$F_{\text{unkn}}(x) = \frac{1}{N}\sum_{i=1}^{N} I(x_{\text{unkn,i}}) \tag{34}$$

where the indicator function $I(\cdot)$ is defined by

$$I(x_{\text{unkn,i}}) = \begin{cases} 1 & \text{if } x_{\text{unkn,i}} < x \\ 0 & \text{otherwise} \end{cases} \tag{35}$$

At each of the MCS simulations, we used a numerical solver to solve the system of equations for the inverse simulation in step (3).

Tables 1 and 2 show the CDFs, $F_{\text{unkn},1}(x)$ and $F_{\text{unkn},2}(x)$, of v_{A0} and v_{B0}, respectively, obtained from the proposed method. The MCS solutions are also shown in the tables.

Table 1. CDF of the initial velocity of body *A* $F_{\text{unkn},1}(x)$

	x (m/s)	New method	MCS
1	7.50	0.0007	0.0007
2	7.95	0.0072	0.0073
3	8.40	0.0372	0.0372
4	8.85	0.1146	0.1148
5	9.30	0.2459	0.2467
6	9.75	0.4090	0.4098
7	10.20	0.5709	0.5717
8	10.65	0.7073	0.7081

9	11.10	0.8095	0.8100
10	11.55	0.8802	0.8807
11	12.0	0.9263	0.9266
12	12.45	0.9552	0.9552
13	12.90	0.9729	0.9728
14	13.35	0.9836	0.9838
15	13.80	0.9900	0.9901
16	14.25	0.9939	0.9939
17	14.70	0.9962	0.9962
18	15.15	0.9976	0.9976
19	15.60	0.9985	0.9985
20	16.05	0.9990	0.9991
21	16.50	0.9994	0.9994

Table 2. CDF of the initial velocity of body *B* $F_{\mathrm{unkn},2}(x)$

	x (m/s)	New method	MCS
1	0.090	0.0009	0.0010
2	0.2555	0.0090	0.0089
3	0.4210	0.0433	0.0431
4	0.5865	0.1261	0.1262
5	0.7520	0.2596	0.2601
6	0.9175	0.4201	0.4203
7	1.0830	0.5766	0.5770
8	1.2485	0.7079	0.7087
9	1.4140	0.8069	0.8076
10	1.5795	0.8762	0.8766
11	1.7450	0.9221	0.9225
12	1.9105	0.9516	0.9516
13	2.0760	0.9700	0.9700
14	2.2415	0.9814	0.9815
15	2.4070	0.9885	0.9886
16	2.5725	0.9928	0.9928
17	2.7380	0.9954	0.9954
18	2.9035	0.9971	0.9971
19	3.0690	0.9981	0.9981
20	3.2345	0.9988	0.9988
21	3.40	0.9992	0.9992

The means, μ_1 and μ_2, and standard deviations, σ_1 and σ_2, of v_{A0} and v_{B0}, are also provided in Table 3. The solutions of the proposed method are close to those from MCS.

Table 3. Means and standard deviations

	Proposed method	MCS
μ_1 (m/s)	10.1594	10.1555
μ_2 (m/s)	1.0631	1.0626
σ_1 (m/s)	1.2211	1.2074
σ_2 (m/s)	0.4615	0.4586

Table 4 gives the numbers of direct simulations by the proposed method for the CDF estimation at all the points shown in Tables 1 and 2. The numbers are between 25 and 40 for the CDF evaluations. The corresponding numbers are much higher by MCS. Since the number of MCS is 19.3463×10^7 and the number of simulations is 10^7, the average number of direct simulations by each MCS simulation is $19.3463\times10^7/10^7=19.3$. The first column in the table gives the indexes of the discrete points in the horizontal axes of Fig. 6 and 7.

Table 4. Number of direction simulations

	Proposed method for v_{A0}	Proposed method for v_{B0}	MCS
1	30	30	19.3463×10^{7}
2	30	30	19.3463×10^{7}
3	30	30	19.3463×10^{7}
4	35	25	19.3463×10^{7}
5	36	31	19.3463×10^{7}
6	34	34	19.3463×10^{7}
7	43	42	19.3463×10^{7}
8	36	36	19.3463×10^{7}
9	35	31	19.3463×10^{7}
10	30	30	19.3463×10^{7}
11	30	35	19.3463×10^{7}
12	30	30	19.3463×10^{7}
13	30	30	19.3463×10^{7}
14	30	35	19.3463×10^{7}
15	35	35	19.3463×10^{7}
16	35	30	19.3463×10^{7}
17	35	35	19.3463×10^{7}
18	35	35	19.3463×10^{7}
19	40	25	19.3463×10^{7}
20	40	35	19.3463×10^{7}
21	40	40	19.3463×10^{7}

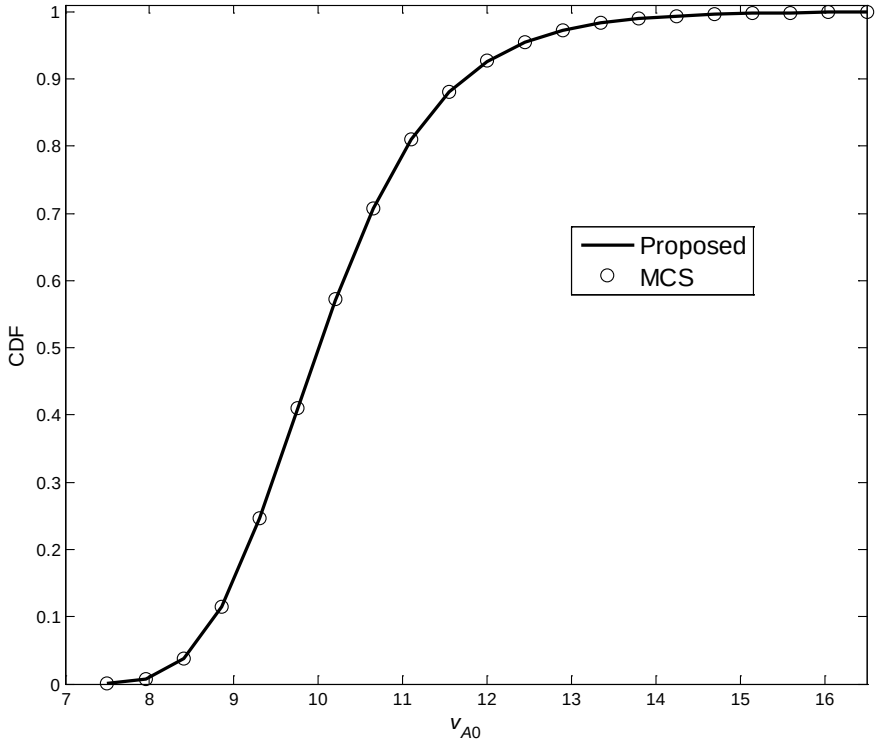

Figure. 6 CDF of the velocity of body *A* before impact

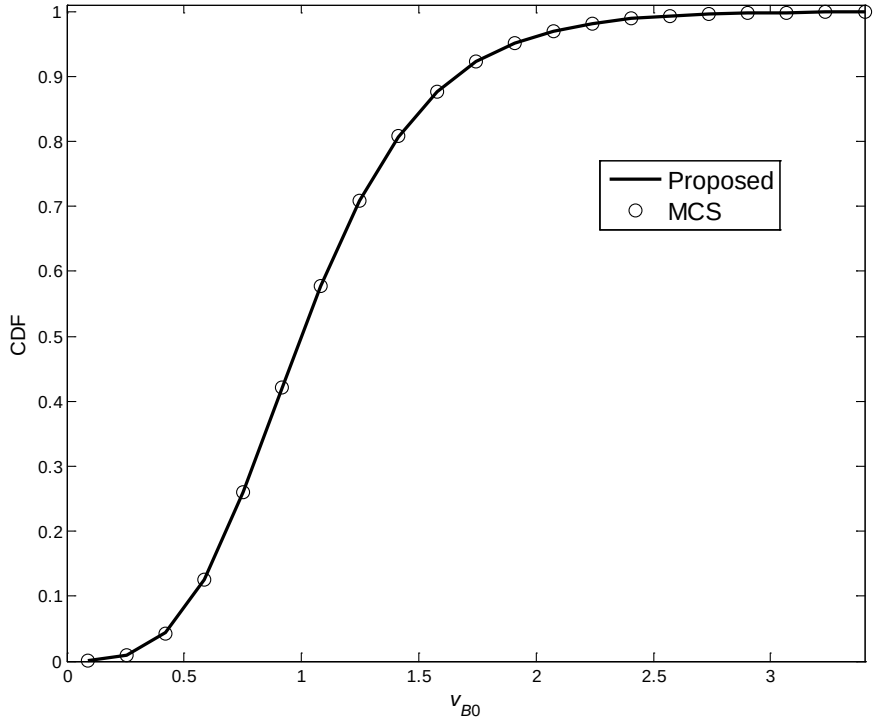

Figure. 7 CDF of the velocity of body *B* before impact

In this example, the unknown input variables are obtained in the form of probability distributions even though their specific values exist. The reason is that the specific values or the realizations of the random known input variables are not available. The uncertainties in the random known input variables result in the uncertainties in inverse simulation results.

5. DISCUSSIONS AND CONCLUSIONS

Inverse simulation has been widely used in industry, and its applications are inevitably surrounded by many uncertainties. To make inverse simulation be more

confidently used, we need to assess the effects of uncertainty on the inverse simulation results. For this purpose, this work integrates the First Order Reliability Method (FORM), which is one of the most important uncertainty analysis methodologies, with inverse simulation. The integration is computationally efficient because the inverse simulation iteration is completely combined with the reliability analysis iteration. The overall inverse simulation under uncertainty is performed by a single-loop procedure.

The example involves only independently and normally distributed random variables; the present methodology, however, can also deal with dependent and non-normal distributions.

In this work, we considered the inverse simulation problems where the realizations of the random input variables are not available. In reality, the realizations may exist. If the realizations are available, the random input known variables will be deterministic for a given set of output variables. In this case, the proposed methodology should be modified.

We also assume, in this work, that uncertainties only exist in some of the model input variables. In reality, however, uncertainties may also be associated with the known model output variables. For example, measurement uncertainties are encountered if model output variables are obtained from measurement. As a result, some of the output variables also need to be treated as random variables. The present methodology can be extended to situations where both input and output variables are random. The methodology can even be further extended to applications where the model structure uncertainty must be included.

The FORM-based methodology in this work shares the same advantages and drawbacks as original FORM. It is efficient but may not be accurate for highly nonlinear

simulation models. If higher accuracy is desired, the Second Order Reliability Method (SORM) can be used. For the CDF estimation, FORM can be easily replaced by SORM. We can first apply the proposed method to obtain an MPP without any modifications. Then we perform an addition analysis, which is the evaluation of the second derivatives of the unknown variables at the MPP. Using the second derivatives will improve the accuracy of the CDF estimation. The evaluation of the mean and standard deviation by SORM, however, needs a further investigation because the extension of the FORM-based method is not straightforward.

ACKNOWLEDGMENT

This material is based upon the work supported by the National Science Foundation under Grant No. CMMI 1234855. The author would also like to acknowledge the helpful discussions with Dr. Xiaoyun Zhang from Shanghai Jiaotong University regarding traffic accident reconstruction simulation.

REFERENCES

[1] Lu, L., 2007, "Inverse Modelling and Inverse Simulation for System Engineering and Control Applications," Ph.D. thesis, University of Glasgow.

[2] Murray-Smith, D. J., 2011, "Feedback Methods for Inverse Simulation of Dynamic Models for Engineering Systems Applications," Mathematical and Computer Modelling of Dynamical Systems, 17(5), pp. 515-541.

[3] Thomson, D., and Bradley, R., 2006, "Inverse Simulation as a Tool for Flight Dynamics Research-Principles and Applications," Progress in Aerospace Sciences, 42(3), pp. 174-210.

[4] Celi, R., 2000, "Optimization-Based Inverse Simulation of a Helicopter Slalom Maneuver," Journal of Guidance, Control, and Dynamics, 23(2), pp. 289-297.

[5] Öström, J., 2007, "Enhanced Inverse Flight Simulation for a Fatigue Life Management System," AIAA Modeling and Simulation Technologies Conference and Exhibit, Hilton Head, South Carolina, August 08, 2007 - August 23, 2007.

[6] Doyle, S. A., and Thomson, D. G., 2000, "Modification of a Helicopter Inverse Simulation to Include an Enhanced Rotor Model," Journal of Aircraft, 37(3), pp. 536-538.

[7] De Divitiis, N., 1999, "Inverse Simulation of Aeroassisted Orbit Plane Change of a Spacecraft," Journal of Spacecraft and Rockets, 36(6), pp. 882-889.

[8] Pontonnier, C., and Dumont, G., 2009, "Inverse Dynamics Method Using Optimization Techniques for the Estimation of Muscles Forces Involved in the Elbow Motion," International Journal on Interactive Design and Manufacturing, 3(4), pp. 227-236.

[9] Tsai, M. S., and Yuan, W. H., 2010, "Inverse Dynamics Analysis for a 3-Prs Parallel Mechanism Based on a Special Decomposition of the Reaction Forces," Mechanism and Machine Theory, 45(11), pp. 1491-1508.

[10] Paul, R. P., 1981, *Robot Manipulators: Mathematics, Programming, and Control: The Computer Control of Robot Manipulators*, The MIT Press,

[11] Matsui, Y., Hitosugi, M., and Mizuno, K., 2011, "Severity of Vehicle Bumper Location in Vehicle-to-Pedestrian Impact Accidents," Forensic Science International, 212(1-3), pp. 205-209.

[12] Steffan, H., 2009, "Accident Reconstruction Methods," Vehicle System Dynamics, 47(8), pp. 1049-1073.

[13] Xiaoyun, Z., Xianlong, J., Xianghai, C., and Xinyi, H., 2011, "The Simulation and Optimization Integration Calculation Method and Application Validation for the Traffic Accident," Advances in Engineering Software, 42(6), pp. 387-397.

[14] Xiaoyun, Z., Xianlong, J., Xianghai, C., and Xinyi, H., 2011, "The First Collision Point Position Identification Method in Vehicle-Pedestrian Impact Accident," International Journal of Crashworthiness, 16(2), pp. 181-194.

[15] Du, X., and Chen, W., 2000, "Methodology for Managing the Effect of Uncertainty in Simulation-Based Design," AIAA journal, 38(8), pp. 1471-1478.

[16] Du, X., and Chen, W., 2002, "Efficient Uncertainty Analysis Methods for Multidisciplinary Robust Design," AIAA Journal, 40(3), pp. 545-552.

[17] Du, X., Sudjianto, A., and Chen, W., 2004, "An Integrated Framework for Optimization under Uncertainty Using Inverse Reliability Strategy," Journal of Mechanical Design, 126(4), pp. 562-570.

[18] Gu, X., Renaud, J. E., Batill, S. M., Brach, R. M., and Budhiraja, A. S., 2000, "Worst Case Propagated Uncertainty of Multidisciplinary Systems in Robust Design Optimization," Structural and Multidisciplinary Optimization, 20(3), pp. 190-213.

[19] Chen, W., Jin, R., and Sudjianto, A., 2005, "Analytical Variance-Based Global Sensitivity Analysis in Simulation-Based Design under Uncertainty," Journal of Mechanical Design, 127(5), pp. 875-886.

[20] Oberkampf, W. L., Deland, S. M., Rutherford, B. M., Diegert, K. V., and Alvin, K. F., 2002, "Error and Uncertainty in Modeling and Simulation," Reliability Engineering and System Safety, 75(3), pp. 333-357.

[21] Kokkolaras, M., Mourelatos, Z. P., and Papalambros, P. Y., 2006, "Design Optimization of Hierarchically Decomposed Multilevel Systems under Uncertainty," Journal of Mechanical Design, 128(2), pp. 503-508.

[22] Youn, B. D., Xi, Z., and Wang, P., 2008, "Eigenvector Dimension Reduction (Edr) Method for Sensitivity-Free Probability Analysis," Structural and Multidisciplinary Optimization, 37(1), pp. 13-28.

[23] Zou, T., Cai, M., Du, R., and Liu, J., 2012, "Analyzing the Uncertainty of Simulation Results in Accident Reconstruction with Response Surface Methodology," Forensic Science International, 216(1–3), pp. 49–60.

[24] Wach, W., and Unarski, J., 2007, "Uncertainty of Calculation Results in Vehicle Collision Analysis," Forensic Science International, 167(2-3), pp. 181-188.

[25] Lee, I., Choi, K. K., and Gorsich, D., 2009, "System Reliability-Based Design Optimization Using the Mpp-Based Dimension Reduction Method," Structural and Multidisciplinary Optimization, pp. 1-17.

[26] Tu, J., Choi, K. K., and Park, Y. H., 1999, "A New Study on Reliability-Based Design Optimization," Journal of Mechanical Design, 121(4), pp. 557-564.

[27] Hohenbichler, M., and Rackwitz, R., 1982, "First-Order Concepts in System Reliability," Structural Safety, 1(3), pp. 177-188.

[28] Der Kiureghian, A., Lin, H.-Z., and Hwang, S.-J., 1987, "Second-Order Reliability Approximations," Journal of Engineering Mechanics, 113(8), pp. 1208-1225.

[29] Du, X., 2008, "Saddlepoint Approximation for Sequential Optimization and Reliability Analysis," Journal of Mechanical Design, 130(1), pp. 101006-1 - 101006-8.

[30] Du, X., 2010, "System Reliability Analysis with Saddlepoint Approximation," Structural and Multidisciplinary Optimization, 42(2), pp. 193-208.

[31] Du, X., and Sudjianto, A., 2004, "First-Order Saddlepoint Approximation for Reliability Analysis," AIAA Journal, 42(6), pp. 1199-1207.

[32] Wong, F. S., 1985, "First-Order, Second-Moment Methods," Computers and Structures, 20(4), pp. 779-791.

Appendix: Simulation Model of the Impact Problem

The *x*- and *y*-components of the velocity of body *A* after impact immediately are

$$v_{Ax} = \frac{(m_A - em_B)v_{A0}\cos\theta - m_B(1+e)v_{B0}}{m_A + m_B} \tag{36}$$

$$v_{Ay} = v_{A0}\sin\theta \tag{37}$$

Then the magnitude of the velocity is

$$v_A = \sqrt{v_{Ax}^2 + v_{Ay}^2} \tag{38}$$

The velocity of body *B* after impact immediately is

$$v_B = v_{Ax} + e(v_{A0}\cos\theta + v_{B0}) \tag{39}$$

The distance d_B is given by

$$d_B = \frac{1}{2g} \frac{v_B^2}{\sin\theta + \mu\cos\theta} \tag{40}$$

where g is the gravitational acceleration.

The distance d_A is given by

$$d_A = v_A \cos\alpha t \tag{41}$$

where

$$\alpha = \arctan(v_{Ay} \,/\, v_{Ax}) + \theta \tag{42}$$

and t is the root of the following equation

$$\frac{1}{2} g t^2 + \big(v_A \sin\alpha\big) t - h = 0 \tag{43}$$

List of table captions

List of figure captions

Table 1. CDF of the initial velocity of body *A* $F_{\mathrm{unkn},1}(x)$

	x (m/s)	New method	MCS
1	7.50	0.0007	0.0007
2	7.95	0.0072	0.0073
3	8.40	0.0372	0.0372
4	8.85	0.1146	0.1148
5	9.30	0.2459	0.2467
6	9.75	0.4090	0.4098
7	10.20	0.5709	0.5717
8	10.65	0.7073	0.7081
9	11.10	0.8095	0.8100
10	11.55	0.8802	0.8807
11	12.0	0.9263	0.9266
12	12.45	0.9552	0.9552
13	12.90	0.9729	0.9728
14	13.35	0.9836	0.9838
15	13.80	0.9900	0.9901
16	14.25	0.9939	0.9939
17	14.70	0.9962	0.9962
18	15.15	0.9976	0.9976
19	15.60	0.9985	0.9985
20	16.05	0.9990	0.9991
21	16.50	0.9994	0.9994

Table 2. CDF of the initial velocity of body *B* $F_{\mathrm{unkn},2}(x)$

	x (m/s)	New method	MCS
1	0.090	0.0009	0.0010
2	0.2555	0.0090	0.0089
3	0.4210	0.0433	0.0431
4	0.5865	0.1261	0.1262
5	0.7520	0.2596	0.2601
6	0.9175	0.4201	0.4203
7	1.0830	0.5766	0.5770
8	1.2485	0.7079	0.7087
9	1.4140	0.8069	0.8076
10	1.5795	0.8762	0.8766
11	1.7450	0.9221	0.9225
12	1.9105	0.9516	0.9516
13	2.0760	0.9700	0.9700
14	2.2415	0.9814	0.9815
15	2.4070	0.9885	0.9886
16	2.5725	0.9928	0.9928
17	2.7380	0.9954	0.9954
18	2.9035	0.9971	0.9971
19	3.0690	0.9981	0.9981
20	3.2345	0.9988	0.9988
21	3.40	0.9992	0.9992

Table 3. Means and standard deviations

	Proposed method	MCS
μ_1 (m/s)	10.1594	10.1555
μ_2 (m/s)	1.0631	1.0626
σ_1 (m/s)	1.2211	1.2074
σ_2 (m/s)	0.4615	0.4586

Table 4. Number of direction simulations

	Proposed method for v_{A0}	Proposed method for v_{B0}	MCS
1	30	30	19.3463×10^{7}
2	30	30	19.3463×10^{7}
3	30	30	19.3463×10^{7}
4	35	25	19.3463×10^{7}
5	36	31	19.3463×10^{7}
6	34	34	19.3463×10^{7}
7	43	42	19.3463×10^{7}
8	36	36	19.3463×10^{7}
9	35	31	19.3463×10^{7}
10	30	30	19.3463×10^{7}
11	30	35	19.3463×10^{7}
12	30	30	19.3463×10^{7}
13	30	30	19.3463×10^{7}
14	30	35	19.3463×10^{7}
15	35	35	19.3463×10^{7}
16	35	30	19.3463×10^{7}
17	35	35	19.3463×10^{7}
18	35	35	19.3463×10^{7}
19	40	25	19.3463×10^{7}
20	40	35	19.3463×10^{7}
21	40	40	19.3463×10^{7}

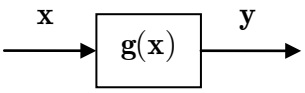

Figure 1. A simulation model

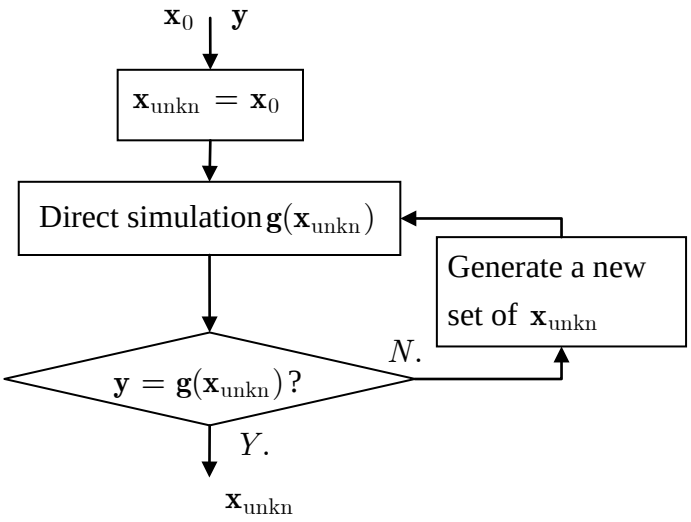

Figure. 2 Flowchart of inverse simulation

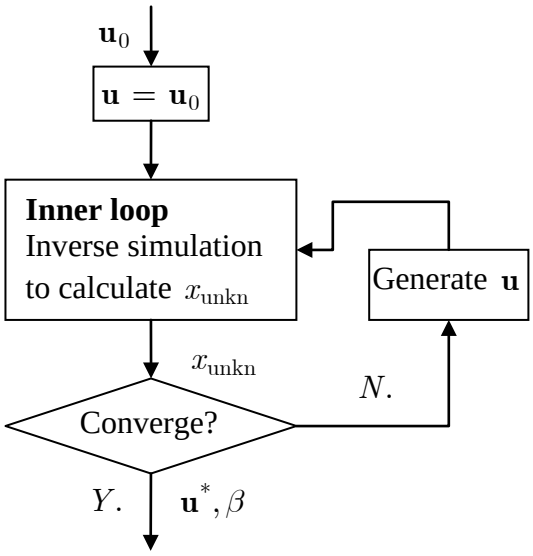

Figure. 3 Double-loop procedure for inverse simulation under uncertainty

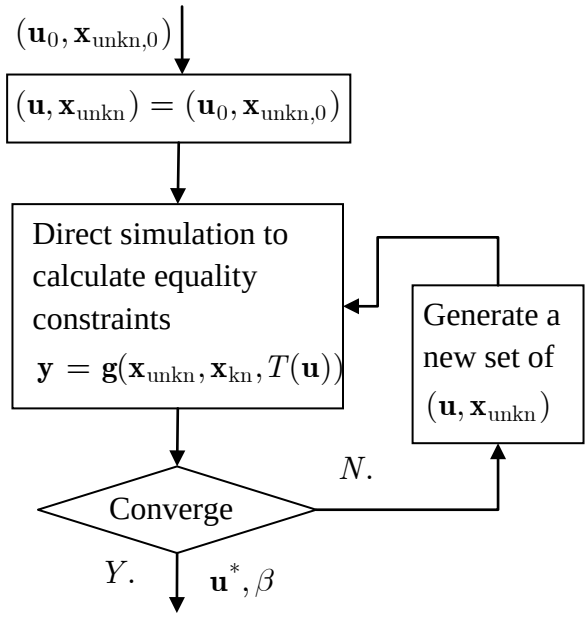

Figure. 4 Single-loop procedure for inverse simulation under uncertainty

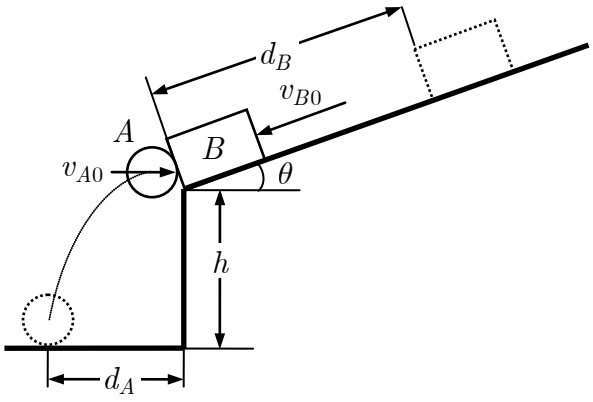

Figure. 5 Impact of two rigid bodies

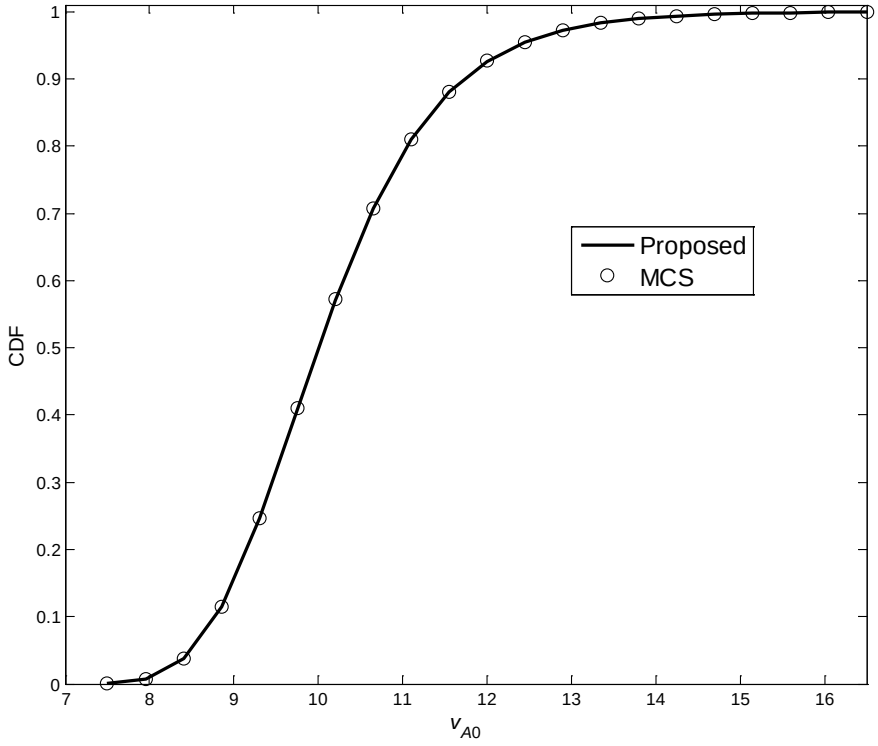

Figure. 6 CDF of the velocity of body *A* before impact

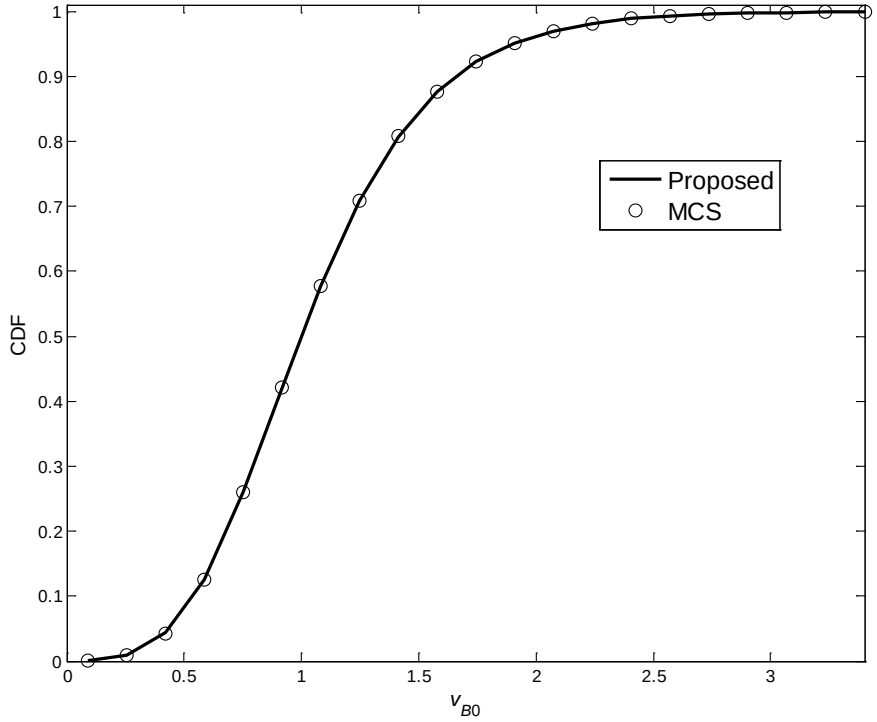

Figure. 7 CDF of the velocity of body *B* before impact